

24. R. J. Keenan, D. M. Freymann, P. Walter, R. M. Stroud, *Cell* **94**, 181 (1998).
25. W. M. Clemons Jr., K. Gowda, S. D. Black, C. Zwieb, V. Ramakrishnan, *J. Mol. Biol.* **292**, 697 (1999).
26. The least-squares superposition of backbone α carbons corresponding to the RNA binding region of the bound M domain (*E. coli* residues 376 to 421), *Thermus aquaticus* [Protein Data Bank (PDB) accession number 2ffh], and human M domain (1QB2) were performed with LSQMAN [G. J. Kleywegt and T. A. Jones, *CCP4 Newslett.* **31**, 9 (1994)]. The backbone root mean square deviation (rmsd) between the *E. coli* and *T. aquaticus* M domains is 0.68 Å, and 0.66 Å between the *E. coli* and human M domains.
27. R. Wintjens and M. Rooman, *J. Mol. Biol.* **262**, 294 (1996).
28. B. Luisi, in *DNA-Protein: Structural Interactions*, D. M. J. Lilley, Ed. (Oxford Univ. Press, Oxford, 1995), pp. 1–49.
29. Reviewed in D. E. Draper, *J. Mol. Biol.* **293**, 255 (1999).
30. H. Mao, S. A. White, J. R. Williamson, *Nature Struct. Biol.* **6**, 1139 (1999).
31. S. A. Strobel, *Biopolymers* **48**, 65 (1998).
32. Nucleotide analog interference mapping was performed as described [S. P. Ryder and S. A. Strobel, *Methods* **18**, 38 (1999)]. In brief, phosphorothioate-tagged nucleotide analogs were incorporated randomly into the 4.5S RNA at the 5% level by run-off transcription by T7 RNA polymerase. This RNA was 5' ^{32}P end-labeled and incubated with M domain at a concentration of 25 pM under standard binding conditions (23). This reaction was passed through a nitrocellulose filter to select for protein-bound RNA, the retained RNA eluted off the filter, and ethanol precipitated. The RNA pellet was resuspended in 10 μl of doubly distilled H_2O and 10 μl of formamide load buffer, and in parallel with control unselected RNA, the phosphorothioate linkages were cleaved by the addition of 1 μl of 1 mM I_2 -ethanol solution and incubation at 90°C for 1 min. The cleavage products were resolved by electrophoresis on a 12% denaturing polyacrylamide gel. The band intensities were quantified by phosphorimaging and the extent of interference determined as described [S. P. Ryder and S. A. Strobel, *Methods* **18**, 38 (1999)].
33. S. Basu *et al.*, *Nature Struct. Biol.* **5**, 986 (1998).
34. A number of other nucleotide analogs, including 2' deoxyadenosine, diamino purine, inosine, and *N*-methyl guanosine, have also been used, and the results are consistent with the crystal structure.
35. H. Wood, J. Luirink, D. Tollervey, *Nucleic Acids Res.* **20**, 5919 (1992).
36. R. T. Batey, L. Lucast, J. A. Doudna, unpublished data.
37. S. Brown, G. Thon, E. Tolentino, *J. Bacteriol.* **171**, 6517 (1989).
38. R. T. Batey, B. Rha, J. A. Doudna, data not shown.
39. The A39U point mutation in the context of the E4 construct was also tested and failed to support growth.
40. J. D. Miller, H. Wilhelm, L. Gierasch, R. Gilmore, P. Walter, *Nature* **366**, 351 (1993).
41. J. D. Miller, S. Tajima, L. Lauffer, P. Walter, *J. Cell Biol.* **128**, 273 (1995).
42. K. Kurita *et al.*, *J. Biol. Chem.* **271**, 13140 (1996).
43. S. J. Gamblin and S. J. Smerdon, *Curr. Opin. Struct. Biol.* **8**, 195 (1998).
44. J. A. Doudna, *Methods Mol. Biol.* **74**, 365 (1997).
45. Z. Otwinoski and W. Minor, *Methods Enzymol.* **276**, 307 (1997).
46. A. T. Brunger *et al.*, *Acta Crystallogr. D* **54**, 905 (1998).
47. T. A. Jones, J. Y. Zou, S. W. Cowan, Kjelsgaard, *Acta Crystallogr. A* **47**, 110 (1991).
48. R. J. Laskowski, M. W. MacArthur, D. S. Moss, J. M. Thornton, *J. Appl. Crystallogr.* **26**, 283 (1993).
49. M. Carson, *J. Appl. Crystallogr.* **24**, 958 (1991).
50. A. Nicholls, K. A. Sharp, B. Honig, *Proteins* **11**, 281 (1991).
51. We thank S. Brown for providing the 4.5S RNA conditionally deficient strains of *E. coli* and helpful advice; C. Ogata for time and assistance at beamline X4A of the National Synchrotron Light Source, Brookhaven National Laboratory; T. Earnest for support at beamline 5.0.2 of the Advanced Light Source, Lawrence Berkeley National Laboratory; R. Hanna, J. Kieft, A. Luptak, and M. Talavera for help with beamline data collection and useful discussions; P. Adams and L. Rice for assistance with the refinement; the staff of the Yale Center for Structural Biology for crystallographic and computational support; S. Strobel for providing the nucleotide analogs and for helpful discussions; S. Basu, J. Cate, J. Davis, T. Griffin, J. Ippolito, S. Ryder, P. Scamborova, P. Sigler, and T. Steitz for many helpful discussions; and J. Cate, J. Kieft, V. Rath, and S. Strobel for critically reading the manuscript. We are particularly indebted to A. Ferré-D'Amaré for excellent advice and support throughout this project. This project was funded in part by a postdoctoral fellowship from the Jane Coffin Childs Memorial Fund for Medical Research (R.T.B.), a Howard Hughes Medical Institute (HHMI) summer fellowship (B.R.), and by support from the NIH, HHMI, and the David and Lucile Packard Foundation. J.A.D. is a Fellow of the David and Lucile Packard Foundation and an Assistant Investigator of HHMI. Coordinates of the SRP core and structure factor amplitudes have been deposited in the PDB (accession code 1DUL). Coordinates are also available at www.csb.yale.edu/people/doudna/doudna_people.html.

14 December 1999; accepted 12 January 2000

REPORTS

Three-Layered Atmospheric Structure in Accretion Disks Around Stellar-Mass Black Holes

S. N. Zhang,^{1,2*} Wei Cui,³ Wan Chen,^{4,5} Yangsen Yao,¹ Xiaoling Zhang,¹ Xuejun Sun,¹ Xue-Bing Wu,⁶ Haiguang Xu⁷

Modeling of the x-ray spectra of the Galactic superluminal jet sources GRS 1915+105 and GRO J1655-40 reveals a three-layered atmospheric structure in the inner region of their accretion disks. Above the cold and optically thick disk with a temperature of 0.2 to 0.5 kiloelectron volts, there is a warm layer with a temperature of 1.0 to 1.5 kiloelectron volts and an optical depth around 10. Sometimes there is also a much hotter, optically thin corona above the warm layer, with a temperature of 100 kiloelectron volts or higher and an optical depth around unity. The structural similarity between the accretion disks and the solar atmosphere suggests that similar physical processes may be operating in these different systems.

The sun has a complicated atmosphere, including a photosphere, a chromosphere, a transition layer, and an outermost hot corona (1, 2). It is generally thought that the magnetic activities of the sun may play an important role in heating the corona (2, 3), although other models have been proposed (4). The atmosphere of the sun is not in hydrodynamical

equilibrium. Consequently, the solar wind is blown outward from the corona. Coronas and outflows are actually common in various types of stellar environments. Here, we present observational evidence and modeling for a solar-type atmosphere for the accretion disks around stellar-mass black holes in x-ray binaries (5).

One of the common characteristics of black hole binaries is the so-called two-component x-ray and gamma-ray spectrum: a soft black-body-like component at low energies (<10 keV) and a hard power-law-like component at high energies (up to several hundred keV) (6). The soft component is generally attributed to the emission from an optically thick, geometrically thin cold accretion disk, which is often described by the standard α -disk model (7). The hard component is attributed to an optically thin, geometrically thick hot corona in either a plane parallel to the disk or with a spherical geometry above the disk (8). The prototype models were motivated by the studies of the solar corona (9).

Recently, more attention has been paid to

¹Physics Department, University of Alabama in Huntsville, Huntsville, AL 35899, USA. ²Space Sciences Laboratory, NASA Marshall Space Flight Center, SD50, Huntsville, AL 35812, USA. ³Center for Space Research, Massachusetts Institute of Technology, Cambridge, MA 02139, USA. ⁴Department of Astronomy, University of Maryland, College Park, MD 20742, USA. ⁵NASA/Goddard Space Flight Center, Code 661, Greenbelt, MD 20771, USA. ⁶Beijing Astronomical Observatory, Chinese Academy of Sciences, Beijing 100012, People's Republic of China. ⁷Institute for Space and Astrophysics, Department of Applied Physics, Shanghai Jiao-Tong University, Shanghai 200030, People's Republic of China.

*To whom correspondence should be addressed. E-mail: zhangsn@email.uah.edu

REPORTS

the similarities between the physical processes in accretion disks and those in the sun, because the empirically invoked viscosity for the disks might have originated from the same dynamo processes operating on the sun (10). Consequently, like in the sun, magnetic turbulence and buoyancy may trigger magnetic flares high above the disks that could cause intense in situ particle heating and acceleration, thus powering a disk corona (11). The relative importance of the soft and hard spectral components in black hole binaries is probably modulated by the energy deposition in the corona by magnetic flares (12)—more energy deposited in the corona produces a stronger hard component. It was proposed that there also exists a layer between the corona and the cold accretion disk, which is directly responsible for the observed soft component (13, 14).

To explore the structure of accretion disks in black hole binaries, we modeled the x-ray spectra of two such sources, GRO J1655-40 and GRS 1915+105, both of which are galactic superluminal jet sources (15). It has been suggested that the higher-than-normal temperature of the soft component of the two sources is caused by the rapid spin of the black holes in these systems, which results in the disk extending closer to the black hole horizon (16, 17). Here, we report the results based primarily on data collected from the Japanese-U.S. x-ray satellite ASCA (Advanced Satellite for Cosmology and Astrophysics), which has good energy resolution and effective area in the 0.7- to 10-keV energy band, which are ideal for studying the soft component.

For black hole binaries, x-ray emission is powered by the release of gravitational energy of matter being accreted by the central black holes, which occurs mostly in the inner region of the accretion disks. Because electron scattering dominates over free-free absorption in the inner disk (7), the emergent x-ray spectrum is fully Comptonized (a photon must undergo many scattering events before escaping). The inner disk region is also dominated by radiation pressure (as opposed to gas pressure), and thus its temperature (T) changes slowly with radius (r) [$T(r) \propto 1/r^{3/8}$] (8), as opposed to a more rapid temperature variation in the gas pressure-dominated disk [$T(r) \propto 1/r^{3/4}$] (8). Therefore, we can approximate the emergent x-ray spectrum from the disk as the Comptonization of a single-temperature blackbody spectrum by an electron cloud (18). In the standard α -disk model, the cloud has the same temperature as the x-ray emission and its optical depth is very large (>100) (8).

For this analysis, we adopted the Comptonization model by Titarchuk (18) and fit it with the observed spectra to determine these key parameters, including the blackbody temperature of the seed photons (the original photons before the Compton scattering), the electron temperature, and the optical depth of the cloud

Table 1. Results for all ASCA observations of GRO J1655-40 and GRS 1915+105; simultaneous CGRO and RXTE data were also used for determining the high-energy component above 10 keV. In about half of the observations, the high-energy component is detectable or dominating the total luminosity.

Observation*	N_{H}^{\dagger} (10^{22} H/cm 2)	Soft component				Hard component			
		kT_0 (keV)	kT_e (keV)	τ	$F_{x\ddagger}$	kT_0 (keV)	kT_e (keV)	τ	$F_{x\ddagger}$
A/94/08/23	0.26	0.20	1.56	8.1	0.32				
A/95/08/15	0.39	0.21	1.21	12.3	2.1				
A/97/02/26	0.57	0.33	1.02	12.8	5.9	1.31	>95	<0.01	1.7
A/94/09/27	0.56	0.26	0.94	14.4	4.8	0.92	>47	<1.0	0.1
B/94/09/27	3.45	0.33	1.31	12.7	1.8				
B/95/04/20	3.55	0.51	1.42	13.8	3.4				
B/96/10/23	3.82	0.46	1.10	8.1	2.0	1.06	>87	<0.2	2.9
B/97/04/25	3.60	0.46	1.11	8.9	1.0	1.07	>35	<0.8	1.4
B/98/04/04	3.57	0.45	1.06	9.7	1.0	1.12	>26	<1.0	1.3

*A, GRO J1655-40; B, GRS 1915+105. Dates are given as YY/MM/DD. $\dagger N_{\text{H}}$, interstellar neutral hydrogen column density. \ddagger The unabsorbed flux (F_x) is in units of 10^{-8} erg cm $^{-2}$ s $^{-1}$. kT_0 , seed-photon temperature of the Comptonization process; kT_e , electron temperature of the Comptonization medium; τ , optical depth of the Comptonization medium.

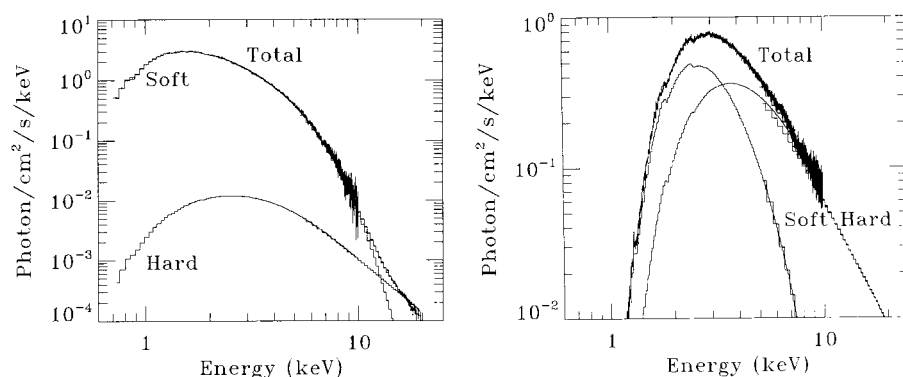


Fig. 1. Sample spectra of (left) GRO J1655-40 observed on 25 February 1997 and (right) GRS 1915+105 observed on 23 October 1996. Both soft and hard components are important in these spectra. ASCA data: 0.7 to 10 keV; RXTE data: 5 to 20 keV (RXTE data above 20 keV are not shown for clarity).

(Table 1). This model fits the data well for cases in which the hard component is negligible. When the hard component is important, a second Comptonized component is required. Although we use the same Comptonization model for the soft and hard spectral components, the physical environments for the two are different: The hard component is produced in an optically thin hot corona (about 100 keV or 10^9 K), whereas the soft component is produced in an optically thick warm cloud (about 1 keV or 10^7 K). As an example, we plotted the results from spectral modeling of GRO J1655-40 and GRS 1915+105 (Fig. 1).

For the soft component, the results indicate that the temperature of the electron cloud is higher than the effective temperature of the seed photons to the Comptonization process, by a factor of three to six, and the inferred optical depth of the cloud (~ 10) is much smaller than that expected from the standard α -disk model (>100). These results provide observational evidence for the presence of a lower density, warm layer outside the standard cold disk. The hard spectral component, on the other hand, cannot be well constrained by the ASCA data

alone because the electron temperature of the Comptonizing corona is higher than the upper end of the ASCA band (10 keV). However, the temperature of the corona can be estimated with the data obtained with the high-energy instruments of CGRO (the U.S. Compton Gamma-Ray Observatory) and RXTE (the U.S. Rossi X-ray Timing Explorer). Using the high-energy CGRO (20 to 500 keV) and RXTE (5 to 250 keV) data obtained simultaneously with the ASCA observations, we found that the corona has a temperature of 100 keV or higher and an optical depth on the order of unity or less (Table 1). These findings agree with numerous previous reports on the high-energy spectra of these two sources [for example, (16, 19, 20)]. The temperature of seed photons for the high-energy Comptonization process is similar to that of the warm layer (Table 1). This implies that the main source of seed photons feeding the corona is the emergent Comptonized spectrum from the warm layer outside the cold disk. The contribution of the hard component to the total x-ray luminosity varies, from being negligible to being dominant, so the corona is a dynamic environment. At the same time, the warm layer

REPORTS

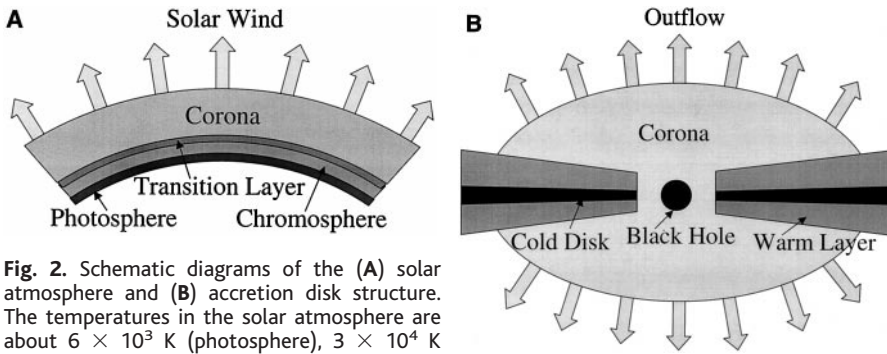


Fig. 2. Schematic diagrams of the (A) solar atmosphere and (B) accretion disk structure. The temperatures in the solar atmosphere are about 6×10^3 K (photosphere), 3×10^4 K (chromosphere), and 2×10^6 K (corona). For the black hole disk atmosphere, the corresponding temperatures are about 500 times as high: 3×10^6 K (cold disk), 1.5×10^7 K (warm layer), and 1×10^9 K (corona).

does not seem to vary appreciably. It is possible that the layer between the cold disk and the hot corona in Cyg X-1 (14) and the ionized cloud in GRO J1655-40 and GRS 1915+105 inferred from the iron absorption features (21) in some of the data we used here are in fact the warm layer we identified. However, this warm layer is not produced by the heating of the corona (14), because of the apparent independence between the relatively stable warm layer and the highly dynamical corona, which sometimes disappears completely.

Although we used a thermal Comptonization model (the electron kinetic energy is assumed to follow the Maxwellian distribution) in our fitting, it is worth pointing out that nonthermal electron energy distribution (for the high-energy spectral component) may also be consistent with the data, as implied by steep power-law spectra extending beyond several hundred keV in some observations (20). In this case, the electron temperature inferred in our model fitting should be considered the lower limit to the kinetic energy of electrons in the corona. Therefore, the corona may also be in the form of jets or outflow from the black hole or near-spherical converging flow into the black hole (22). Current x-ray data alone do not allow us to distinguish these different coronal geometries unambiguously.

The inferred structure of accretion disks of black hole binaries can be compared with the structure of the solar atmosphere (Fig. 2). The photosphere, chromosphere, and corona of the sun appear to correspond to the surface of the cold disk, the overlying optically thick warm layer, and the optically thin hot corona, respectively. The transition region between the chromosphere and the corona in the solar atmosphere, however, could not be identified in disks from our current spectral fitting. It cannot correspond to the warm layer, because the latter is observed even in the absence of the corona (the hard component). The temperatures of the three regions are higher in the accretion disks by about a factor of 500 than the corresponding regions in the sun. This supports the notion that magnetic activity is responsible for powering the upper atmosphere in both cases, giving $T \propto$

$E^{1/4} \propto B^{1/2}$ and thus $T_{\text{DISK}}/T_{\text{SUN}} \approx (B_{\text{DISK}}/B_{\text{SUN}})^{1/2} \approx (10^8 \text{ G}/500 \text{ G})^{1/2} \approx 500$, where E is the total energy radiated, B is the strength of the magnetic field, T_{DISK} is the temperature of the disk, T_{SUN} is the temperature of the sun, B_{DISK} is the strength of the magnetic field in the inner accretion disk region, and B_{SUN} is the strength of the magnetic field in the active regions of the solar surface.

Because the solar wind is driven out primarily by strong coronal activities, by analogy, we argue that the corona surrounding accretion disks of black hole binaries is also a source of outflow. In fact, a recent accretion disk model suggests that magnetic field-driven jets and outflow are also important in the angular momentum transfer, which is essential in order for the accretion process to operate in these systems (23). The connection between corona and outflow is also supported by the fact that radio emissions from black hole binaries seem to always be accompanied by the detection of substantial hard x-ray emission (19). Although the magnetic fields may be generated by the dynamo processes as a result of the differential rotation in both the sun and the accretion disks of black hole binaries (1), the two types of systems are different. In the sun, the source of radiation energy is the nuclear burning in the core, and only a small portion of the total energy is converted to the magnetic field. In accretion disks, however, all radiation energy comes from the viscous dissipation of gravitational energy, which may originate in magnetic turbulence (10). It is, therefore, natural that the magnetic field-related energy dissipation in accretion disks is more important than that in the sun. Consequently, our results provide support to theoretical predictions that relativistic jets and outflow from these systems are magnetic field driven (24). In fact, it has been realized recently that there might exist a "magnetic switch" in these systems; when the magnetic field activity exceeds a certain limit, fast and relativistic jets may be produced (25). Our results reported here and the fact that GRO J1655-40 and GRS 1915+105 have been observed to produce highly relativistic jets (15) provide support to this

magnetic switch theory. The disk coronas powered by magnetic flares are also believed to exist in the accretion disks around supermassive black holes (11). Therefore, similar physical processes may operate in systems with different properties and scales.

References and Notes

1. T. Tajima and K. Shibata, *Plasma Astrophysics*, vol. 98 of *Frontiers in Physics* (Addison-Wesley, Reading, MA, 1997).
2. E. R. Priest, in *Solar and Stellar Activity: Similarities and Differences*, vol. 158 of *ASP Conference Series*, C. J. Butler and J. G. Doyle, Eds. (Astronomical Society of the Pacific, San Francisco, CA, 1999), pp. 321-333.
3. P. A. Sturrock, *Astrophys. J.* **521**, 451 (1999).
4. J. D. Scudder, *Astrophys. J.* **398**, 319 (1992).
5. P. Charles, in *Theory of Black Hole Accretion Disks*, M. A. Abramowicz, G. Bjornsson, J. E. Pringle, Eds. (Cambridge Univ. Press, Cambridge, 1998), pp. 1-20.
6. W. H. G. Lewin and Y. Tanaka, in *X-ray Binaries*, W. H. G. Lewin, J. van Paradijs, E. P. J. van den Heuvel, Eds. (Cambridge Univ. Press, Cambridge, 1995), pp. 457-494; S. N. Zhang et al., in *Proceedings of the Fourth Compton Symposium*, vol. 410 of *AIP Conference Proceedings 141* (American Institute of Physics, New York, 1997), pp. 141-162; J. van Paradijs, in *The Many Faces of Neutron Stars*, R. Buccheri, J. van Paradijs, M. A. Alpar, Eds. (Kluwer Academic, Dordrecht, Netherlands, 1998), pp. 279-336.
7. N. I. Shakura and R. A. Sunyaev, *Astron. Astrophys.* **24**, 337 (1973).
8. E. P. Liang, *Phys. Rep.* **302**, 67 (1998).
9. ——— and R. H. Price, *Astrophys. J.* **218**, 247 (1977).
10. J. F. Hawley, S. A. Balbus, W. F. Winters, *Astrophys. J.* **518**, 394 (1999).
11. F. Haardt, L. Maraschi, G. Ghisellini, *Astrophys. J.* **476**, 620 (1997).
12. T. Di Matteo, A. Celotti, A. C. Fabian, *Mon. Not. R. Astron. Soc.* **304**, 809 (1999).
13. S. Nayakshin and F. Melia, *Astrophys. J.* **490**, L13 (1997).
14. R. Misra, V. R. Chitnis, F. Melia, *Astrophys. J.* **495**, 407 (1998).
15. I. F. Mirabel and L. F. Rodriguez, *Nature* **371**, 46 (1994); S. J. Tingay et al., *Nature* **374**, 141 (1995); R. M. Hjellming and M. P. Rupen, *Nature* **375**, 464 (1995); I. F. Mirabel and L. F. Rodriguez, *Nature* **392**, 673 (1998).
16. S. N. Zhang et al., *Astrophys. J.* **479**, 381 (1997).
17. S. N. Zhang, W. Cui, W. Chen, *Astrophys. J.* **482**, L155 (1997); W. Cui, S. N. Zhang, W. Chen, *Astrophys. J.* **492**, L53 (1998).
18. R. A. Sunyaev and L. G. Titarchuk, *Astron. Astrophys.* **143**, 374 (1985); L. Titarchuk, *Astrophys. J.* **434**, 570 (1994).
19. B. A. Harmon et al., *Nature* **374**, 703 (1995); B. A. Harmon et al., *Astrophys. J.* **477**, L85 (1997).
20. J. E. Grove et al., *Astrophys. J.* **500**, 899 (1998); J. A. Tomsick, P. Kaaret, R. A. Kroeger, R. A. Remillard, *Astrophys. J.* **512**, 892 (1999).
21. Y. Ueda et al., *Astrophys. J.* **492**, 782 (1998).
22. S. Chakrabarti and L. G. Titarchuk, *Astrophys. J.* **455**, 623 (1995); K. Borozdin, M. Revnivtsev, S. Trudolyubov, C. Shrader, L. Titarchuk, *Astrophys. J.* **517**, 367 (1999).
23. R. D. Blandford and M. C. Begelman, *Mon. Not. R. Astron. Soc.* **303**, L1 (1999).
24. R. D. Blandford and D. G. Payne, *Mon. Not. R. Astron. Soc.* **199**, 883 (1982).
25. D. L. Meier, S. Edgington, P. Godon, D. G. Payne, K. R. Lind, *Nature* **388**, 350 (1997); D. L. Meier, *Astrophys. J.* **522**, 753 (1999).
26. We thank J. You, R. Shelton, A. Harmon, K. Ghosh, and L. Titarchuk for useful discussions and K. Ebisawa for help on ASCA data analysis. We acknowledge partial financial support from NASA Goddard Space Flight Center under the Long Term Space Astrophysics program and several guest investigations and from NASA Marshall Space Flight Center through contract NCC8-65.

3 November 1999; accepted 4 January 2000